Inverse scattering designs of dispersion-engineered single-mode planar waveguides

Alexander R. May, Francesco Poletti, Michalis N. Zervas
Optoelectronics Research Centre, University of Southampton, Southampton, SO17 1BJ

ABSTRACT

We use an inverse-scattering (IS) approach to design single-mode waveguides with controlled linear and higher-order dispersion. The technique is based on a numerical solution to the Gelfand-Levitan-Marchenko integral equation, for the inversion of rational reflection coefficients with arbitrarily large number of leaky poles. We show that common features of dispersion-engineered waveguides such as trenches, rings and oscillations in the refractive index profile come naturally from the IS algorithm without any a priori assumptions. Increasing the leaky-pole number increases the dispersion map granularity and allows design of waveguides with identical low order and differing higher order dispersion coefficients.

Keywords: Inverse-scattering, dispersion-engineered, planar waveguides

1. INTRODUCTION

Since the development of the erbium-doped fiber amplifier (EDFA) there has been increased interest in in-fiber devices that provide low loss, high reliability and compatibility with the transmission line. These devices have found a variety of applications ranging from signal conditioning in the form of amplification and dispersion control, to network management in the form of multiplexing and/or network monitoring[1]. While the control of dispersion in optical fibers is often associated with dispersion compensation in optical communications networks[2] there is also interest in its control for the purposes of harnessing nonlinear optical effects. Parametric processes[3] and supercontinuum generation[4] rely upon tailoring of the dispersion profile of the fiber to enhance energy transfer and thus time has been spent over the last several decades to develop technologies to fine control waveguide dispersion[5].

Silica-based highly nonlinear fibers (HNLF) feature very low attenuation loss-characteristics and so by using long lengths of these fibers a large nonlinear effect can be realized. Small mode effective areas and thereby large nonlinearity are produced by increasing the refractive index difference between the core and the cladding which enhances the confinement of the light. This may be achieved by utilizing a highly germanium-doped core and a fluorine-doped cladding. In addition to creating a small mode effective area, nonlinear processes such as four-wave mixing (FWM) require the pump wavelength to coincide with the zero-dispersion wavelength of the fiber. Further control of the dispersion slope is advantageous in controlling dispersion and increasing operating bandwidth.

In principle the wave equations and boundary conditions governing the modal properties of a fiber are analogous to the wave function of a particle in a box often considered in quantum mechanics. As such a typical dispersion-engineered fiber with a given refractive index distribution can be considered to be a potential distribution with three discrete segments – a core and a ring with an index greater than silicon that attracts light and a depressed index trench which acts as a barrier. The index and thickness of these regions determines the rate as a function of wavelength at which the mode transitions from the core to the ring, and it is this as well as the average refractive index in which the light exists that controls the propagation constant and its derivatives and thereby the dispersion properties of the fiber.

While the dispersion-engineering of fibers is typically approached through a trial and error method and parametric study, authors[6,7,8,9,10,11] have in the past studied the design of planar waveguides as well as fibers from the point of view of inverse-scattering (IS). Here the modal properties of the waveguide are specified at the start of the process and through the inverse design process the waveguide with these properties is obtained. In this paper, as a starting point to a more general analysis with fibers, we describe the dispersion characteristics of IS designed planar waveguides. We begin with an overview of IS theory before considering design cases for which exact solutions exist which have previously

been discussed in the literature, before extending this to a set of new cases. We then show that typical dispersion-engineered waveguide features such as rings and trenches come naturally from this theory. We finally discuss what benefits the new extended cases bring to the literature.

2. INVERSE SCATTERING THEORY

If we consider a planar optical waveguide with a varying refractive index $n(x)$ surrounded by two cladding layers of constant index n_2 as shown in Figure 1, it may support TE modes that are assumed to be of the form

$$E_y(x,z,t) = E_{y0}(x,k_0)\exp(i\beta z)\exp(-i\omega t) \tag{1}$$

where z is the direction of propagation, ω is the frequency, β is the propagation constant along the z-axis and k_0 is the free-space wave number. The vector wave equations reduce to the form

$$\frac{d^2E_y}{dx^2} + \left[k_0{}^2 n(x)^2 - \beta^2\right]E_y = 0 \tag{2}$$

which can be rewritten as a Schrodinger equation

$$\frac{d^2E_y}{dx^2} + \left[k^2 - q(x)\right]E_y = 0 \tag{3}$$

with transverse propagation constant k in the cladding and the potential $q(x)$ of the form

$$q(x) = k_0{}^2\left[n_2{}^2 - n(x)^2\right] \tag{4}$$

The refractive index profile $n(x)$ of an optical waveguide is determined from its transverse reflection coefficient $r(k)$ through the solution of the Gelfand-Levitan-Marchenko (GLM) integral equation[12] for the unknown kernel $K(x,t)$ [7]

$$R(x+t) + K(x,t) + \int_{-t}^{x} K(x,y)R(x+y)dy = 0 \tag{5}$$

where $x \geq |t|$, and the reflected transient $R(t)$ is given as[7],

$$R(t) = \frac{1}{2\pi}\int_{-\infty}^{\infty} r(k)\exp(-ikt)dk - i\sum_{p=1}^{n} r_p \exp(-ik_p t) \tag{6}$$

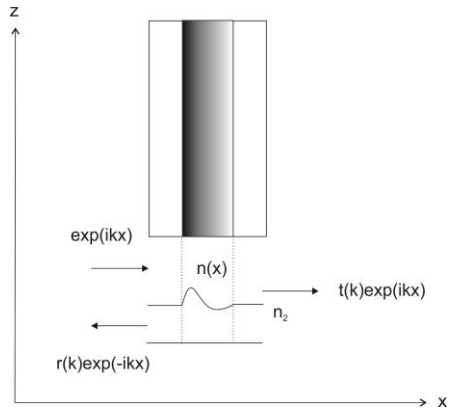

Figure 1. The physical model for electromagnetic reflection from an inhomogeneous planar waveguide

The reflection coefficient $r(k)$ is a rational function, of which poles k_p on the positive imaginary axis correspond to guided modes with corresponding residues r_p. As such the integral in the above expression corresponds to the continuous spectrum of radiation modes, while the sum to the discrete set of guided modes[7,13]. Once the kernel $K(x,t)$ has been obtained, the potential is then derived from the relation[7]

$$q(x) = 2\frac{dK(x,x)}{dx} \tag{7}$$

and the refractive index profile in turn from

$$n(x) = \sqrt{n_2^{\,2} - \frac{q(x)}{k_0^{\,2}}} \tag{8}$$

A general reflection coefficient can be approximated by a rational reflection coefficients[14] and so we begin our study by considering three, five and seven-pole rational reflection coefficients. In particular, previous authors have investigated the three pole case using analytic expressions and the complexity of these increases quickly with the increase in number of poles. In view of Galois' proof that 5th and higher-order polynomial equations are insoluble by radicals, the semi-analytical numerical technique of Pechenick[15] provides a welcome alternative. It is also worth noting that this is to our knowledge the first time this technique has been applied to wave-guiding structures.

3. WAVEGUIDE DESIGNS

In this section we describe the inverse scattering designs obtained using three-pole, five-pole and seven-pole rational reflection coefficients. We first demonstrate that the IS method of Pechenick[15] correctly generates the three-pole wide-core waveguide first considered by Lakshmanasamy and Jordan[6] while also demonstrating that associated with the three pole parameter space (which is limited in domain by the requirement of conservation-of-energy) is a waveguide dispersion map. It is shown that this parameter space may be extended further than previously explored to generate increasingly dispersive designs. We then move further by considering five-pole and seven-pole rational reflection coefficients for which firstly the allowable parameter space is identified computationally using Sturm's Theorem[16] whereby we evaluate the existence of roots of a higher order conservation-of-energy condition than originally introduced for the three-pole case in Appendix A of Jordan and Lakshmanasamy[7] and secondly the dispersion maps are obtained

showing that dispersion can be tailored about a three-pole design point. All waveguides designs are truncated at ten microns.

3.1 Three-pole rational reflection coefficients

The waveguide designs associated with the three-pole rational reflection coefficients are of the form

$$r(k) = \frac{k_1 k_2 k_3}{(k-k_1)(k-k_2)(k-k_3)} \tag{9}$$

with poles k_1, k_2, k_3 for which $c_1, c_2 \in R^+$

$$\begin{aligned} k_1 &= -c_1 - ic_2 \\ k_2 &= c_1 - ic_2 \\ k_3 &= i \end{aligned} \tag{10}$$

As in the existing literature the conjugate symmetric poles k_1 and k_2 are representative of the radiation modes and are termed 'leaky poles', while k_3 represents a guided mode at a propagation constant of $|k_3| = 1\ \mu\text{m}^{-1}$.

In order for a solution to exist, the reflection coefficient must obey a set of conditions[17] which are satisfied by the general form given in (9). Conservation of energy, $r(k) \le 1$ for all real k, dictates that the parameter space is limited. Previous authors[6,7] have identified and considered the allowable region bounded above by the line $c_2 = 0.5$ and to the right by the lemniscate of Bernoulli[17]. The allowable region can be extended past these points as is illustrated in Figure 2 below which shows the dispersion D_2, dispersion slope D_3 and dispersion curvature D_4 associated with the allowable region.

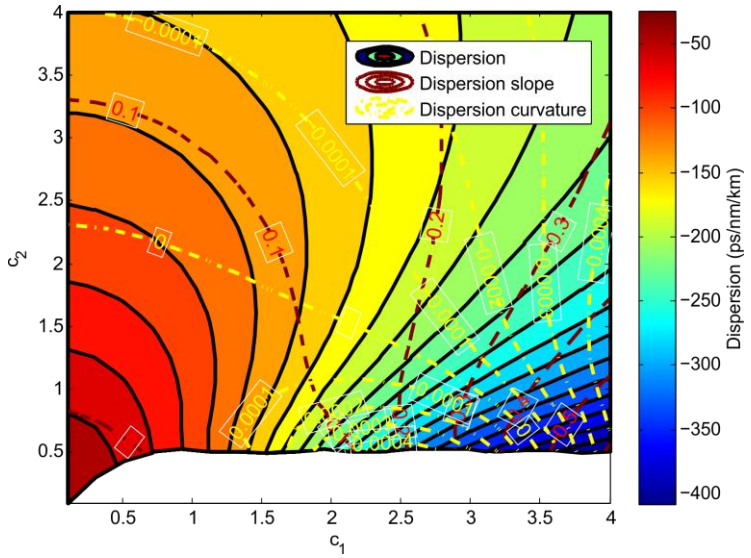

Figure 2. The allowable three-pole parameter space showing contours of dispersion, dispersion slope and dispersion curvature assuming cladding index $n_2 = 1.444$ and design wavelength $\lambda = 1.55\mu\text{m}$

It can be seen that leakier poles lead to waveguides with greater dispersion indicated by the movement from red in the lower left hand side to green to blue in the lower right hand side. Dispersion slope and a more negative dispersion curvature are also found to occur. Two illustrative examples are those obtained for the pole positions in the parameter space previously considered by Lakshmanasamy and Jordan[6] and shown in Figure 3. Here we see that the leakier poles in the design associated with the red curve result in features loosely resembling a W-type refractive index profile and larger dispersion. On the other hand, designs with small leaky poles such as those depicted by the blue curve more closely resemble a step-index design.

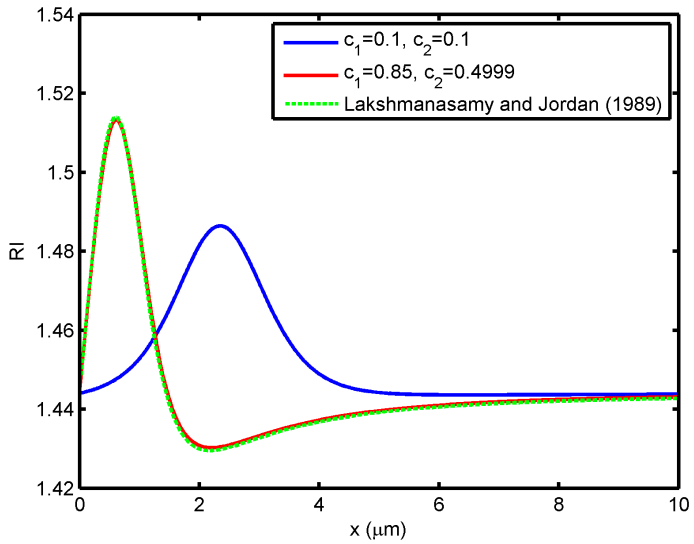

Figure 3. Refractive index profiles for the inner and outer limit of the parameter space previously considered by Lakshmanasamy and Jordan [6] with $n_2 = 1.444$ and $\lambda = 1.55\mu$m , and the exact design obtained by Lakshmanasamy and Jordan[6]

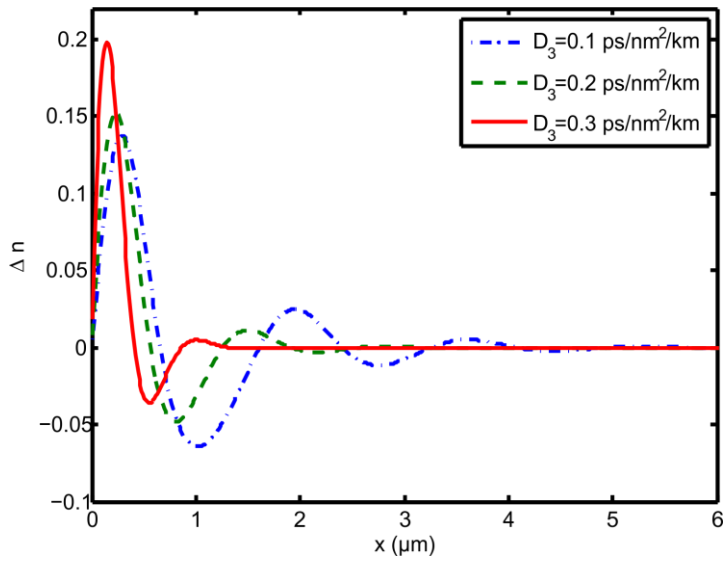

Figure 4. Waveguide designs for which $D_2 = -215$ ps/nm/km and D_3 varies from 0.1 ps/nm^2/km to 0.3 ps/nm^2/km , assuming $n_2 = 1.444$ and $\lambda = 1.55\mu$m

We also note that designs exist for which the dispersion is a constant, but the dispersion slope and dispersion curvature differ. As an example we consider the case for which $D_2 = -215$ ps/nm/km but D_3 varies from 0.1 ps/nm^2/km to 0.3 ps/nm^2/km, while we ignore changes in dispersion curvature D_4, as shown in Figure 4.

We observe that increasing the size of the dispersion slope for a constant value of dispersion causes the refractive index to narrow and steepen. It is particularly interesting to note that the design with flattest dispersion slope contains significant trench and ring features, as well as oscillations, the area of which result in a flattening of dispersion slope. The existence of these additional features varies the rate at which the electric field expands into the cladding with increasing wavelength.

In order to better understand the significance of the individual leaky pole parameters c_1 and c_2 we investigated the significance of leaky pole radius on the designs. For two values of this radius R, we varied the pole parameters and obtained Figure 5.

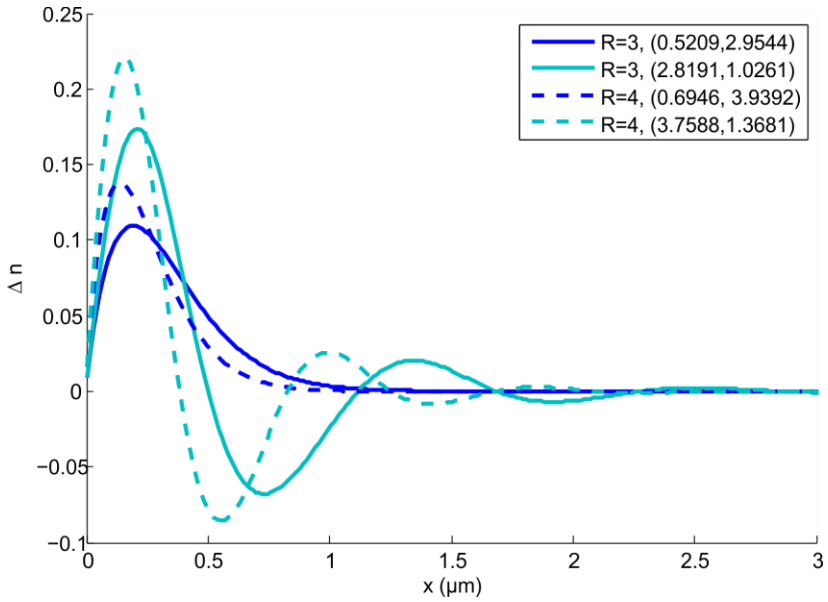

Figure 5. The influence of leaky pole radius R on waveguide design, assuming $n_2 = 1.444$ and $\lambda = 1.55\mu$m

Increasing the leaky pole radius does in all cases result in a narrowing and steepening of the design as is seen when comparing the filled and dotted curves. However, it is the size of the c_1 parameter that is most influential in developing trenches, rings and oscillations.

To further investigate the effect of variation in c_1 for constant c_2 we plotted Figure 6 which shows that increasing c_1 decreases the period of oscillation from the green curve to the cyan curve. It is also interesting to note that a more oscillatory design is associated with a more distorted reflection response $r(k)$ as seen in Figure 7.

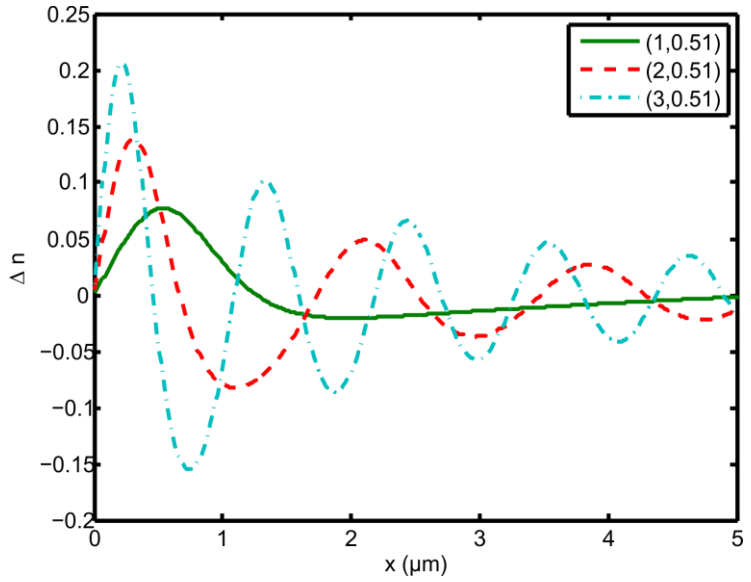

Figure 6. The variation in oscillation period with c_1 for a fixed $c_2 = 0.51$, assuming $n_2 = 1.444$ and $\lambda = 1.55\mu$m

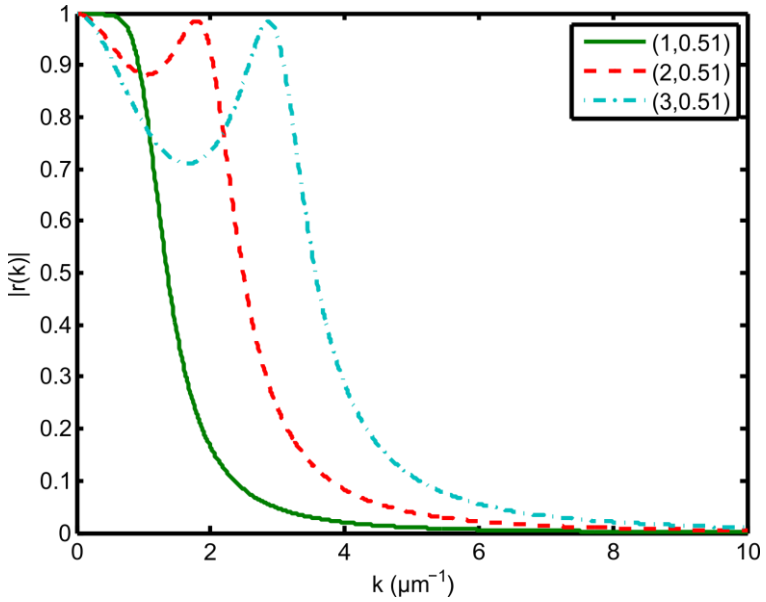

Figure 7. The variation in $r(k)$ with c_1 for a fixed $c_2 = 0.51$

3.2 Five-pole and seven-pole rational reflection coefficients

We may proceed further and explore rational reflection coefficients with five poles of the form

$$r(k) = \frac{k_1 k_2 k_3 k_4 k_5}{(k-k_1)(k-k_2)(k-k_3)(k-k_4)(k-k_5)} \tag{11}$$

where for $c_1, c_2, d_1, d_2 \in R^+$

$$\begin{aligned} k_1 &= -c_1 - ic_2,\ k_2 = c_1 - ic_2 \\ k_3 &= -d_1 - id_2, k_4 = d_1 - id_2 \\ k_5 &= i \end{aligned} \tag{12}$$

As has previously been mentioned, it is possible to calculate the allowable values of c_1, c_2, d_1, d_2 that satisfy conservation-of-energy and for which solutions to the inverse scattering problem exist. Here we once again choose the guided mode pole k_5 to correspond to propagation at $|k_5| = 1\mu\text{m}^{-1}$ while also choosing the first two poles to be those from the previous three-pole design problem, $k_{1,2} = \pm 0.85 - 0.4999i$. Using Sturm's Theorem the allowable domain of the additional two parameters d_1, d_2 may be found and the dispersion map is shown in Figure 8.

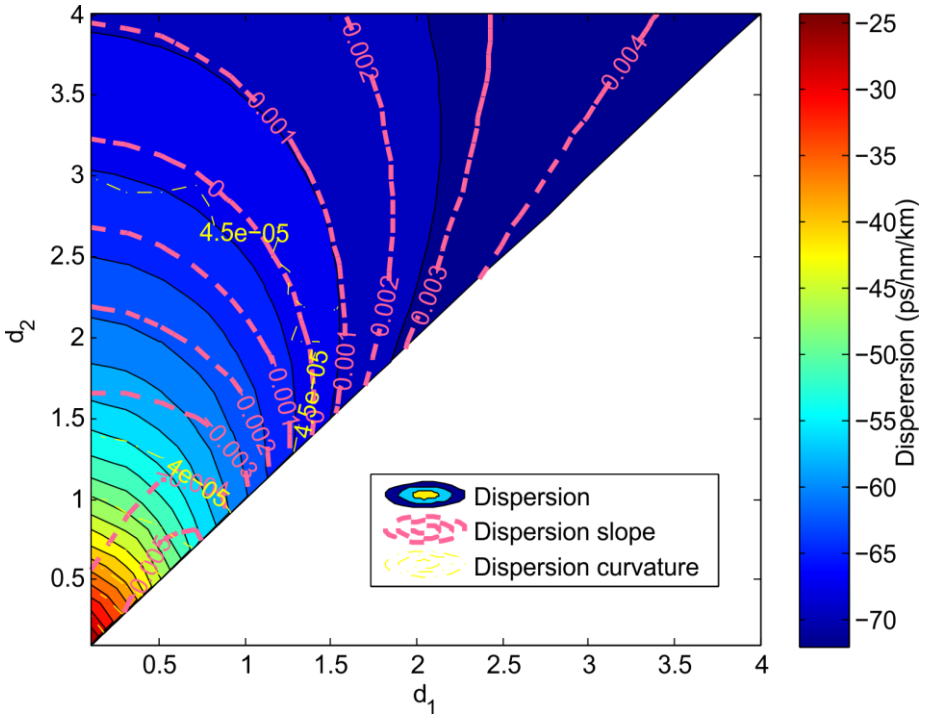

Figure 8. Waveguide dispersion as a function of additional leaky pole positions for a five-pole case assuming $(c_1, c_2) = (0.85, 0.4999)$, $|k_5| = 1\mu\text{m}^{-1}$, $n_2 = 1.444$ and $\lambda = 1.55\mu\text{m}$

We first notice from Figure 8 that the dispersion of these five-pole designs is limited in magnitude by the size of the initial leaky pole parameters c_1, c_2 to a value of the order of $D_2 = -70$ ps/nm/km while at the same time increasing the overall allowable domain. If we repeat this procedure but this time assuming $(c_1, c_2) = (2 \times 0.85, 2 \times 0.4999)$ we obtain the allowable region and dispersion map given in Figure 9.

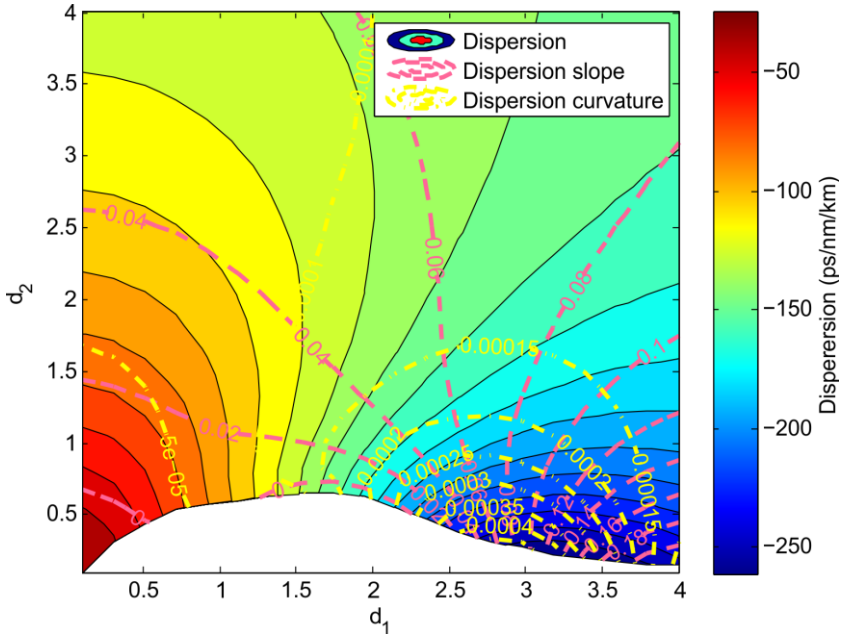

Figure 9. Waveguide dispersion as a function of additional leaky pole positions for a five-pole case assuming $(c_1, c_2) = (2\times 0.85, 2\times 0.4999)$, $|k_5| = 1\mu\text{m}^{-1}$, $n_2 = 1.444$, $\lambda = 1.55\mu\text{m}$

Once again the dispersion has been limited to values of the order found for the initial three pole case of Figure 2. From this we deduce that the addition of poles leads to increased granularity in the design process. That is, it is possible to range over similar orders of dispersion, dispersion slope and dispersion curvature as you find located at the values of c_1 and c_2 in the three-pole cases but with a more gradual change in waveguide design. From a practical point of view we can arbitrarily take a three-pole design with waveguide dispersion $D_2 = -261$ ps/nm/km and dispersion slope $D_3 = 0.13$ ps/nm^2/km, find a five-pole design with these very same second and third order characteristics but show that the dispersion curvature differs. This is shown in Figure 10.

Table 1. Three, five and seven-pole designs with significantly differing dispersion slope, assuming $n_2 = 1.444$, $\lambda = 1.55\mu\text{m}$ and $c_1 = 2\times 0.85$, $c_2 = 2\times 0.4999$, $d_1 = c_1 + \Delta$, $d_2 = c_2 + \Delta$, $e_1 = d_1 + \Delta$, $e_2 = d_2 + \Delta$, $\Delta = 0.01$

Design	Dispersion D_2	Dispersion slope D_3	Dispersion curvature D_4
Three-pole	–145 ps/nm/km	7.98×10^{-2} ps/nm^2/km	1.02×10^{-4} ps/nm^3/km
Five-pole	–132 ps/nm/km	2.26×10^{-2} ps/nm^2/km	1.52×10^{-4} ps/nm^3/km
Seven-pole	–120 ps/nm/km	-8.48×10^{-3} ps/nm^2/km	1.12×10^{-4} ps/nm^3/km

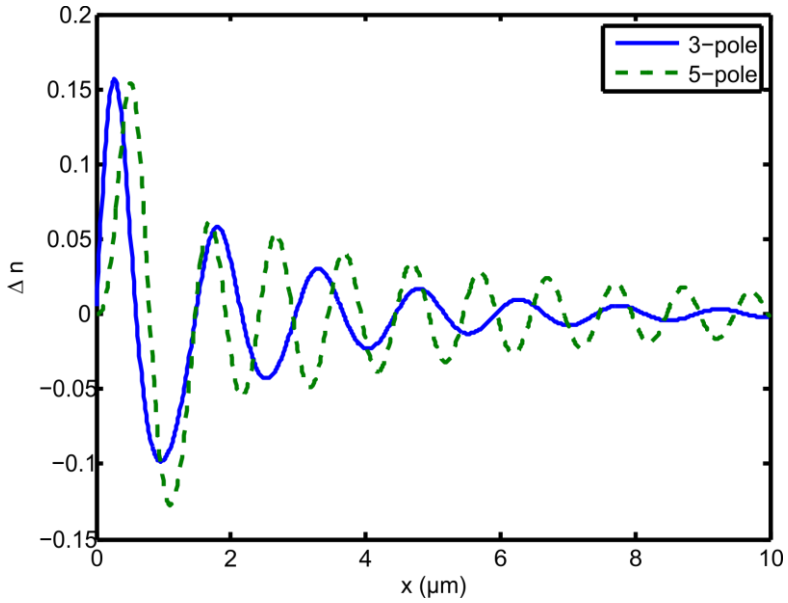

Figure 10. Three pole $(c_1, c_2) = (2.2775, 0.52692)$ and five pole designs $(c_1, c_2, d_1, d_2) = (2\times0.85, 2\times0.4999, 3.1789, 0.22485)$ with identical $D_2 = -261$ ps/nm/km , $D_3 = 0.130$ ps/nm^2/km but differing $D_4 = 4.41\times10^{-4}$ ps/nm^3/km and $D_4 = 4.29\times10^{-4}$ ps/nm^3/km , assuming $n_2 = 1.444$, $\lambda = 1.55\mu$m

Of additional interest is the fact that if the pole positions are chosen to all be located in the same neighborhood but with displacement Δ , thus avoiding multiplicity which would void the inverse-scattering technique[17], then the three-pole, five-pole and seven-pole cases demonstrate similar values of waveguide dispersion D_2 and dispersion curvature D_4 but significant reduction of dispersion slope as shown in Table 1. Associated with this change in dispersion slope is an expansion and exaggeration of the core, ring and trench as shown in Figure 11.

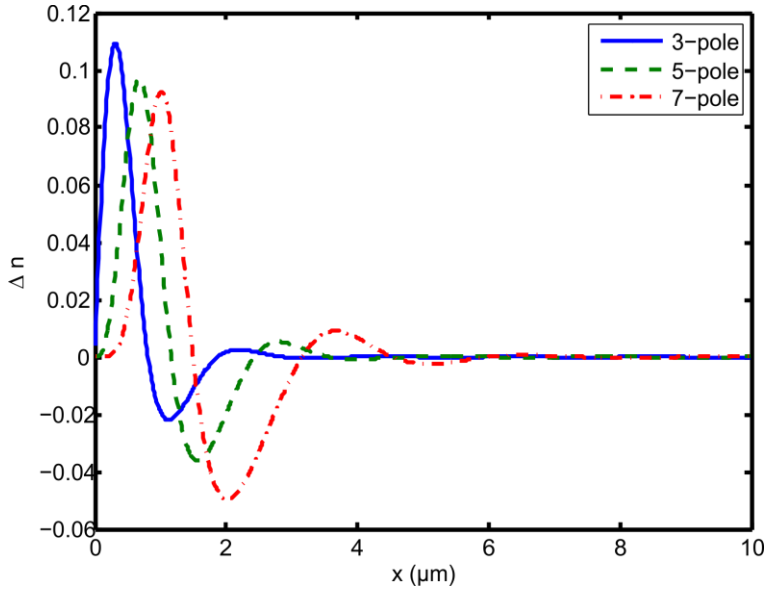

Figure 11. Three, five and seven-pole designs with significantly differing dispersion slope, assuming $n_2 = 1.444$, $\lambda = 1.55\mu$m and $c_1 = 2\times0.85$, $c_2 = 2\times0.4999$, $d_1 = c_1 + \Delta$, $d_2 = c_2 + \Delta$, $e_1 = d_1 + \Delta$, $e_2 = d_2 + \Delta$, $\Delta = 0.01$

4. CONCLUSIONS

In conclusion we have shown that common features of dispersion-engineered waveguides such as trenches, rings and oscillations come naturally from inverse scattering theory when the magnitude of leaky poles in increased. In particular, while the leaky pole radius does lead to increased core size, trench size and dispersive properties, it is the magnitude of the c_1 parameter near the forbidden region of the three-pole case that introduces and controls the period of oscillation in the refractive index profile. Associated with the introduction of oscillations in the refractive index profile is an additional peak in the reflection response $r(k)$ which becomes increasingly accentuated with the c_1 parameter. We have also shown that for the three-pole cases, the allowed parameter space previously used[6] can be extended to one which has previously not been considered for waveguide designs and provides the opportunity for increasingly dispersive designs. The addition of further poles to the inverse scattering procedure, which has also not been investigated previously, has been shown to increase the granularity in the design process about a three-pole dispersion design point. As such, the dispersion obtained from such higher order pole designs is limited by the choice of the initial two poles with c_1 and c_2 dominating the design process while additional poles add complexity to the refractive index profile. This complexity results in differing higher order dispersion.

From a design point of view this work has also for the first time to our knowledge shown that the method developed by Pechenick[15] for the solution of inverse scattering problems involved in ionospheric structure determination can also be used in the design of waveguides. It is of additional interest that we have also for the first time to our knowledge used Sturm's theorem in the determination of the allowed parameter spaces for higher pole designs. In order to fully utilize the increased design complexity and features available from the addition of poles it would be necessary to perform an optimization procedure over the parameter space. We had initially investigated finding a closed-form connection between the pole positions and waveguide dispersion characteristics without the need for solving the forward problem for a true inverse solution to the design problem but this currently remains unsolved. However, we believe that this initial study shows promise for the use of inverse scattering in the understanding and/or design of dispersion-engineered fibers or waveguides and we plan to extend these designs in further papers.

REFERENCES

[1] Ramachandran, S., "Dispersion-Tailored Few-Mode Fibers : A Versatile Platform for In-Fiber Photonic Devices," Journal of Lightwave Technology 23(11), 3426–3443 (2005).

[2] Wandel, M., and Kristensen, P., "Fiber designs for high figure of merit and high slope dispersion compensating fibers," Journal of Optical Fiber Communication 3, 25–60 (2005).

[3] Agrawal, G.P., [Nonlinear Fiber Optics] , Academic Press, London, UK (2001).

[4] Dudley, J.M., and Coen, S., "Supercontinuum generation in photonic crystal fiber," Reviews of Modern Physics 78(4), 1135–1184 (2006).

[5] Takahashi, M., Sugizaki, R., Hiroishi, J., Tadakuma, M., Taniguchi, Y., and Yagi, T., "Low-Loss and Low-Dispersion-Slope Highly Nonlinear Fibers," Journal of Lightwave Technology 23(11), 3615–3624 (2005).

[6] Lakshmanasamy, S., and Jordan, A.K., "Design of wide-core planar waveguides by an inverse scattering method.," Optics Letters 14(8), 411–413 (1989).

[7] Jordan, A.K., and Lakshmanasamy, S., "Inverse scattering theory applied to the design of single-mode planar optical waveguides," Journal of the Optical Society of America A 6(8), 1206–1212 (1989).

[8] Papachristos, C., "Synthesis of single-and multi-mode planar optical waveguides by a direct numerical solution of the Gel'fand-Levitan-Marchenko integral equation," Optics Communications 203, 27–37 (2002).

[9] Hirsh, I., Horowitz, M., and Rosenthal, A., "Design of Planar Waveguides With Prescribed Mode-Profile Using Inverse Scattering Theory," Journal of Quantum Electronics 45(9), 1133–1141 (2009).

[10] Cvijetic, M., "Dual-mode optical fibres with zero intermodal dispersion," Optical and Quantum Electronics 16(4), 307–317 (1984).

[11] Jordan, A.K., and Ahn, S., "Electronics Inverse scattering theory and profile reconstruction," Proceedings of the Institution of Electrical Engineers 126(10), 945–950 (1979).

[12] Kay, I., "The Inverse Scattering Problem When the Reflection Coefficient is a Rational Function," Communications on Pure and Applied Mathematics XIII, 371–393 (1960).
[13] Xia, J., and Jordan, A., "Inverse-scattering view of modal structures in inhomogeneous optical waveguides," JOSA A 9(5), 740–748 (1992).
[14] Reilly, M., and Jordan, a., "The applicability of an inverse method for reconstruction of electron-density profiles," IEEE Transactions on Antennas and Propagation 29(2), 245–252 (1981).
[15] Pechenick, K.R., "Inverse scattering—exact solution of the Gel'fand-Levitan equation," Journal of Mathematical Physics 22(7), 1513–1516 (1981).
[16] Akritas, A., and Vigklas, P., "Counting the number of real roots in an interval with Vincent's theorem," Bull. Math. Soc. Sci. Math. Roumanie 53(3), 201–211 (2010).
[17] Pechenick, K.R., "Exact solutions to the valley problem in inverse scattering," Journal of Mathematical Physics 24(2), 406–409 (1983).